LES-IB Study of Mixing Enhancement by Polygonal Orifices and Wavy Walls

A. Tyliszczak, M. Ksiezyk and Bernard J. Geurts

1 Introduction

Control of mixing in turbulent flow may lead to considerable improvement of efficiency, safety and performance of various technological devices. In so-called passive control methods, shapes of control elements (bluff-bodies, swirlers, etc.) are often a result of trial-and-error based on geometrical modifications.

In the present study we apply passive control to enhance mixing of fuel issuing from a pipe into a hot co-flowing stream. Near the outlet of the pipe plates with polygonal orifices are mounted. The role of these objects is to intensify mixing of large and small scales which potentially will lead to better mixing characteristics between the fuel and co-flow downstream of the pipe exit. We confront the gain in the mixing efficiency inside the pipe with the power required to keep the assumed flow rate. Next we focus on the mixing characteristics downstream the pipe. In particular we look at what happens with the flame as function of the orifice shape.

The research is performed using the LES (Large Eddy Simulation) approach combined with the IB (Immersed Boundary) method. The advantage of the IB method over the classical approach with body-fitted meshes is that flow problems can be solved on Cartesian grids and the objects immersed in the flow domain may be of arbitrary complexity as there is no need to create the mesh around it. The combustion

A. Tyliszczak (✉) · M. Ksiezyk
Department of Mechanical Engineering and Computer Science, Czestochowa University of Technology, Al. Armii Krajowej 21, 42-201 Czestochowa, Poland
e-mail: atyl@imc.pcz.pl

M. Ksiezyk
e-mail: mksiezyk@imc.pcz.pl

B.J. Geurts
Multiscale Modelling and Simulation, University of Twente, Box 217, 7500 AE Enschede, The Netherlands
e-mail: b.j.geurts@utwente.nl

D.G.E. Grigoriadis et al. (eds.), *Direct and Large-Eddy Simulation X*,
ERCOFTAC Series 24, https://doi.org/10.1007/978-3-319-63212-4_46

process is modelled applying the CMC (Conditional Moment Closure) model which allows for analysis of very complex physical phenomena, including auto-iginition and flame lifting which occur in the present study.

2 Modelling and Computational Setup

Governing equations and implementation issues of the LES-CMC approach, together with the solution procedure applied in the present study may be found in [4, 5]. We use an academic LES solver called SAILOR which was previously validated in various studies including wall bounded flows, jet flows and flames [5]. The Navier-Stokes and continuity equations are discretized using a 6th order compact difference method for half-staggered meshes [6]. In the equation for the mixture fraction 5th order WENO (Weighted Essentially Non-Oscillatory) and 6th order compact schemes are used for the convection and diffusion terms, respectively. The time integration employs the Adams-Bashforth / Adams-Moulton predictor-corrector method. Resolutions are such that near-DNS accuracy is achieved.

The CMC equations were solved applying the operator splitting approach where the transport in physical space, transport in mixture fraction space and chemistry are solved separately. The convective terms were discretized using the 2nd order TVD (Total Variation Diminishing) method with van Leer limiters. The diffusive terms were discretised using the central finite difference scheme. The hydrogen chemistry was modelled with the detailed mechanism of Mueller et al. [3] with 9 species and 19 reactions.

The IB method is implemented according to a direct forcing approach [2] which involves adding a source term to the Navier-Stokes equations. Its role is to act on a fluid in such a way as if there were a solid object immersed in the flow domain.

Figure 1 presents the computational configuration used in this study. It corresponds closely to the so-called Cabra flame [1]. The fuel jet is a mixture of hydrogen and nitrogen with molar fraction $X_{H_2} = 0.254$, $X_{N_2} = 0.746$. The fuel temperature is 305K, the mean velocity at the nozzle exit is equal to $U = 107$m/s, and the noz-

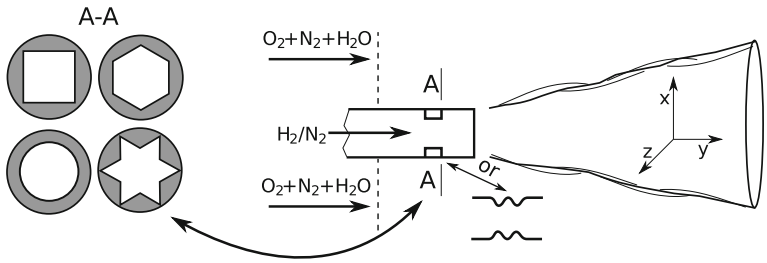

Fig. 1 Schematic view of the test case geometry with shown schematically wavy wall and plates with various orifices (*circle*, *square*, *hexagram*, *hexagon*)

zle diameter is $D = 4.57$mm. The co-flow consists of oxygen $X_{O_2} = 0.147$, water $X_{H_2O} = 0.1$ and nitrogen $X_{N_2} = 0.753$. Its temperature and velocity are equal to $T_c = 1045\text{K}\pm30\text{K}$ and $U_c = 3.5$m/s. We use the geometry and flow conditions of the Cabra flame as reference case which we modify by mounting plates with polygonal orifices or wavy wall upstream of the exit section of the pipe. The shapes of these orifices (circle, square, hexagram, hexagon) are shown in Fig. 1. The length of the plates is taken equal to $L = 0.2D$ and a blockage ratio, i.e., *(Cross-section area of the orifice)/(Cross-section area of the pipe)* to 0.5 for all orifices is used. The length of the wavy wall is $1D$, its shape corresponds to two periods of the sinus function with the amplitude giving the blockage ratio 0.5.

3 Passive Control over Mixing and Combustion

The solution procedure consists of two parts. In the first part the flows inside the pipes is computed as separate problem without considering the flow downstream of the pipes. A time varying velocity component obtained from these simulations is used in the second part of the simulations as the inlet boundary conditions. The velocity signal was extracted from the unsteady 3D results at the cross-section A-A located near the end of the orifices, as shown in Fig. 1, or at the end of the wavy wall.

The simulations were performed at Reynolds numbers equal to $\text{Re} = 1000$ and $\text{Re} = 23{,}600$, with Re defined based on the pipe diameter and inlet velocity. The computations for $\text{Re} = 1000$ were performed to assess accuracy of the applied IB method while the case with $\text{Re} = 23{,}600$ corresponds to the Cabra configuration. It was found that for $\text{Re} = 23{,}600$ the impact of the shape of the orifice is much smaller than at $\text{Re} = 1000$. The flow structures downstream the orifices were very complex, but the velocity contours at a distance of $2D$ behind the plates showed only limited dependence on the orifice shape.

Accuracy of the IB method was verified in test computations performed for two simple orifices, i.e., a circle and a square. As reference results we used the solution obtained with the ANSYS Fluent package and a body-fitted mesh. The dimensions of the computational domain were $6D$ in the axial direction (y) and $1.1D \times 1.1D$ in the perpendicular directions (x, z). Note that in the rectangular domain we not only model the orifices using the IB method but also the walls of the pipe. For the SAILOR code two Cartesian meshes were used with $192 \times 160 \times 160$ and $320 \times 160 \times 160$ nodes compacted axially in the vicinity of the orifices. In the computations performed with Fluent the mesh was matched to the orifices. It consisted of 2.5×10^6 nodes to reach a solution that is quite grid-independent.

Isosurfaces and contours of the instantaneous streamwise velocity obtained in simulations using the IB method at $\text{Re} = 1000$ are presented in Fig. 2. It can be seen that for the circular orifice the flow is ‘smooth’ up to the end of the domain and the only effect of the orifice is a local narrowing of the main stream. The flow through the square orifice is more complex. Behind the corners of the orifice four recirculation regions develop with negative velocities. Close to the outflow elongated structures

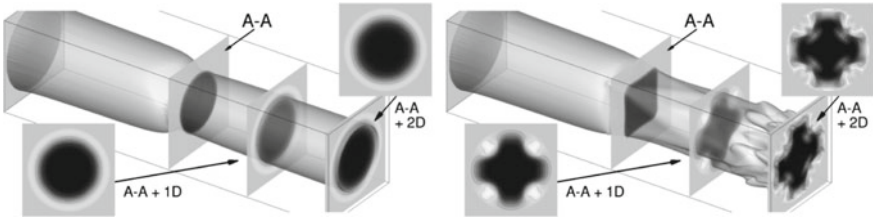

Fig. 2 Isosurface $0.5U$ of instantaneous streamwise velocity and the cross-sections showing its contours ($-0.5U \div 2.5U$) downstream the orifices. Results for circular (*left* figure) and square (*right* figure) orifices with Re = 1000

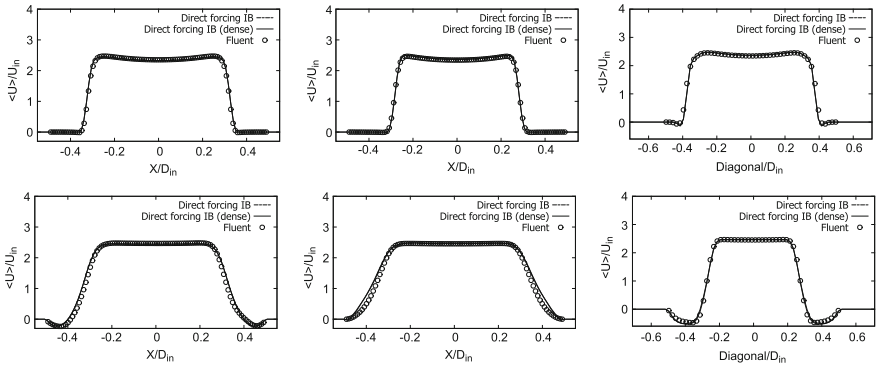

Fig. 3 Profiles of the axial velocity at Re = 1000, for the circular (*left* column) and square orifices (the central and *right* column). *Upper row* location at the A-A cross-section. *Bottom row* $1D$ downstream

form in the corners. In the center of the pipe the flow resembles as if it were issuing from the orifice with a cross shape.

Figure 3 shows profiles of the streamwise velocity at locations corresponding to the end of the plate (upper figures) and also $1D$ downstream (bottom figures). The results for the circular orifice (figures on the left) are presented along the x-direction only while for the square orifice the results are presented along the x-direction (figures in the centre) and along the diagonal direction (figures on the right). The results agree very well with the reference solution. The influence of the mesh density is very small.

The simulations for Re = 23,600 were performed using a mesh with $320 \times 160 \times 160$ nodes. The length of the velocity signals recorded as input boundary data for subsequent simulations was equal to $50D/U$. Figure 4 shows the evolution of the pressure drop along the centerline of the pipe and turbulent kinetic energy $TKE(y)$ integrated over cross-section planes Ω along the pipe with $TKE(y) = \int (u^2_{\mathrm{rms}} + v^2_{\mathrm{rms}} + w^2_{\mathrm{rms}}) \mathrm{d}\Omega$. The level of $TKE(y)$ is used here as indicator of mixing efficiency while the pressure drop is related to the power required to drive the flow at the assumed flow rate. The location of the orifices and wavy wall are also shown in Fig. 4. It is seen that except for the wavy wall the results are quite similar. The largest

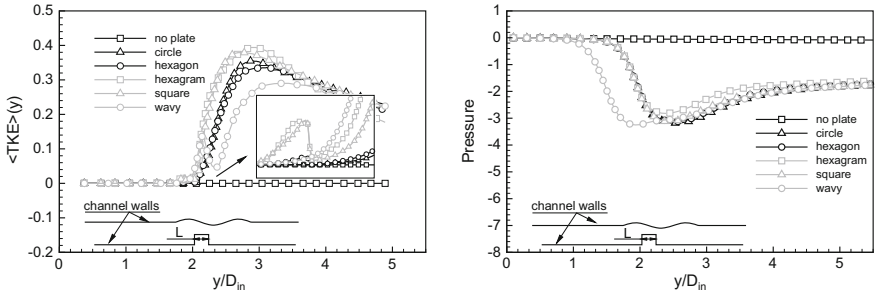

Fig. 4 Profiles of TKE and pressure along the axial direction for Re = 23600

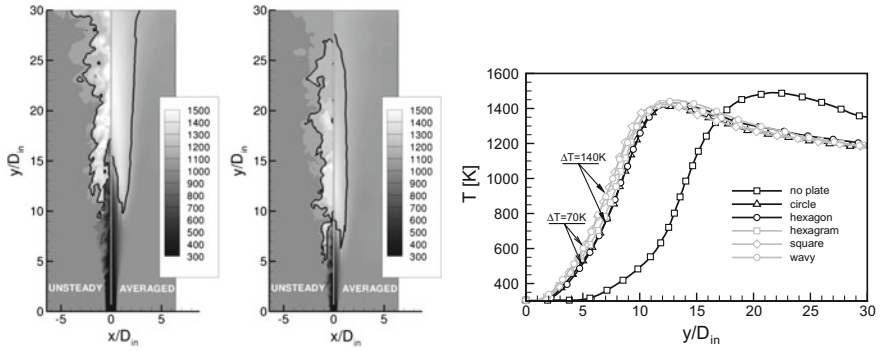

Fig. 5 Contours of instantaneous and time-averaged temperature in the main cross-section plane (two figures on the *left*) and the temperature distribution along the flame axis

$TKE(y)$ is obtained for the square and hexagram orifices. Taking into account that the hexagram orifice leads to the smallest pressure drop this shape seems to be the most efficient, although difference between orifices are small.

In the second part of the simulations combustion is included. The dimensions of the computational domain were increased to $30D \times 14D \times 14D$. The computational grids consisted of $256 \times 160 \times 160$ nodes for the Navier-Stokes equations and $60 \times 21 \times 21$ nodes for the CMC equations. In all analysed cases the flame developed in the domain according to the following scenario. The cold fuel issued from the pipe into the high temperature co-flowing stream and auto-ignited. Auto-ignition spots appeared at axial locations $y > 20D$. Next, the flame quickly spread in the domain, propagated upstream and eventually stabilised a few diameters downstream the inlet. Sample results showing the contours of instantaneous and time-averaged temperature are presented in Fig. 5. These results were obtained for the original Cabra configuration (the left figure) and for the case with the hexagram orifice, where significant difference appear. In the original configuration the lift-off height of the flame (L_H) is approximately $10D$ while in the flame issuing from the hexagram orifice L_H is shortened by 50%. Here, L_H is measured as the distance from the inlet to

the point where the temperature exceeds the co-flow temperature by 1%. Surprisingly, neither the flame shape nor L_H are affected substantially by the type of orifice. This is confirmed by the temperature profiles along the flame axis shown in Fig. 5 on the right hand side. It can be seen that the maximum values are the same for all analysed cases and the maxima are located at $y = 10D - 12D$. Upstream of these locations the fastest temperature growth is obtained for the pipe with wavy wall and square orifice. For instance, compared to the case with the hexagonal orifice, for which the temperature rise is slowest, the temperature difference at $y = 7D$ is approximately 140 K.

4 Conclusions

The present paper showed how LES-IB can be successfully applied to study mixing characteristics in pipes with complex shaped orifice plates. The simulations of flames issuing from such pipes revealed significantly improved mixing which, compared to the flame issuing from a straight pipe, manifested itself by shortening of the lift-off heights of the flames. The results did not show an evident advantage of a particular shape of the orifice. Taking into account that the hexagram shape leads to the smallest pressure drop in the pipe, this shape seems optimal.

Acknowledgements This work has been partially supported by the Polish National Science Center under grant DEC-2012/07/B/ST8/03791 and statutory funds of the Czestochowa University of Technology. The authors are grateful to the computing centres SARA in the Netherlands (NWO project SH-061) and Cyfronet in Poland (computational resources within PL-Grid infrastructure).

References

1. Cabra, R., Myrvold, T., Chen, J.-Y., Dibble, R.W., Karpetis, A.N., Barlow, R.S.: Simultaneous laser Raman-Rayleigh-LIF measurements and numerical modeling results of a lifted turbulent H_2/N_2 jet flame in a vitiated co-flow. Proc. Combust. Inst. **29**, 1881–1888 (2002)
2. Mittal, R., Iaccarino, G.: Immersed boundary methods. Annu. Rev. Fluid Mech. **37**, 239–261 (2005)
3. Mueller, M.A., Kim, T.J., Yetter, R.A., Dryer, F.L.: Flow reactor studies and kinetic modelling of the H2/O2 reaction. Int. J. Chem. Kinet. **31**, 113–125 (1999)
4. Triantafyllidis, A., Mastorakos, E.: Implementation issues of the conditional moment closure in large eddy simulations. Flow Turbul. Combust. **84**, 481–512 (2009)
5. Tyliszczak, A.: Assessment of implementation variants of conditional scalar dissipation rate in LES-CMC simulation of auto. Arch. Mech. **65**, 97–129 (2013)
6. Tyliszczak, A.: A high-order compact difference algorithm for half-staggered grids for laminar and turbulent incompressible flows. J. Comput. Phys. **276**, 438–467 (2014)